ISSN: 2447-3359

REVISTA DE GEOCIÊNCIAS DO NORDESTE

Northeast Geosciences Journal

v. 11, nº 1 (2025)

https://doi.org/10.21680/2447-3359.2025v11n1ID37621

Hydrological study of the Roger dump area in João Pessoa-PB, Brazil

Estudo hidrológico da área do lixão do Roger em João Pessoa-PB, Brasil

Antônio Italcy de Oliveira Júnior[1]; Camila de Melo Tavares[2]; Maria Odete Holanda Mariano[3] José Fernando Thomé Jucá[4]; Mário Augusto Tavares Russo[5]

[1] Universidade Federal de Pernambuco, Departamento de Engenharia Civil e Ambiental, Recife-PE, Brasil. Email: antonio.italcy@ufpe.br
ORCID: https://orcid.org/0000-0002-8297-5068

[2] Universidade Federal de Pernambuco, Departamento de Engenharia Civil e Ambiental, Recife-PE, Brasil. Email: camila.mtavares@ufpe.br
ORCID: https://orcid.org/0000-0002-2470-1480

[3] Universidade Federal de Pernambuco, Departamento de Engenharia Civil e Ambiental, Recife-PE, Brasil. Email: odete.mariano@ufpe.br
ORCID: https://orcid.org/0000-0001-6027-0510

[4] Universidade Federal de Pernambuco, Departamento de Engenharia Civil e Ambiental, Recife-PE, Brasil. Email: jucah@ufpe.br
ORCID: https://orcid.org/0000-0002-8956-7905

[5] Instituto Politécnicode de Viana do Castelo, Viana do Castelo, Portugal. Email: mariorusso@estg.ipvc.pt
ORCID: https://orcid.org/0000-0002-4515-5554

Abstract: The recurrence times or return periods of intense precipitation can be obtained from estimates, making it possible to evaluate the flooding caused by the rise in the water level of water bodies in a region. Such an assessment makes it possible to map water spots and thus verify the areas that could be affected by floods. In this context, this work aimed to evaluate historical precipitation series from pluviometric stations located close to the Lixão do Roger area in João Pessoa-PB, estimate maximum precipitation using continuous probability distribution (Gumbel) for different recurrence times and map the floods generated by these precipitations associated with the recurrence times studied, aiming at safety in the area for the implementation of a park. Using hydrological modeling and delimitation, it was possible to identify the flood areas in the Lixão do Roger area and predict the altitude reached by the flood spots for each recurrence time. For the Cabelo Cagepa Post and considering a recurrence time of 100 years, it is possible to verify that up to 30% of the Lixão do Roger area is affected by floods and the elevation intercepted by the water was approximately 5.87 m

Keywords: Solid waste; Floodable areas; Hydrological mapping.

Resumo: Os tempos de recorrência ou períodos de retorno das precipitações intensas podem ser obtidos a partir de estimativas, sendo possível avaliar a inundação ocasionado pela elevação do nível de água dos corpos d'água de uma região. Tal avaliação possibilita mapear as manchas d'água e assim verificar as áreas que podem ser atingidas pelas inundações. Nesse contexto, este trabalho teve por objetivo avaliar séries históricas de precipitação dos postos pluviométricos situados próximo à área do Lixão do Roger em João Pessoa-PB, estimar as precipitações máximas utilizando distribuição de probabilidade contínua (Gumbel) para diferentes tempos de recorrência e mapear as inundações geradas por estas precipitações associadas aos tempos de recorrência estudados, visando a segurança na área para implantação de um parque. A partir da modelagem hidrológica e da delimitação permitiu identificar as áreas de inundação na área do Lixão do Roger e prever a cota altimétrica atingida pelas manchas de inundação para cada tempo de recorrência. Para o Posto Cabelo Cagepa e considerando um tempo de recorrência de 100 anos é possível verificar que até 30% da área do Lixão do Roger é atingida por inundações e a cota altimétrica interceptada pela água foi de aproximadamente 5,87 m

Palavras-chave: Resíduos sólidos; Áreas inundáveis; Mapeamento hidrológico.

Recebido: 10/09/2024; Aceito: 22/01/2025; Publicado: 04/02/2025.

1. Introduction

The closure of landfill activities reduces the negative environmental impacts caused by their operation. However, deactivation does not eradicate all impacts related to their existence, making it necessary to carry out recovery projects in the deactivated landfill areas (RESENDE et al., 2015).

Recovering a deactivated landfill presents several challenges, from preliminary geotechnical and geophysical studies to more detailed data analyses for possible use of the degraded area. It is essential to evaluate the hydrological processes in the landfill area so that this aspect can be considered when considering a possible use of the degraded area and to avoid future problems with intense rainfall (LISBOA et al., 2016).

Rainfall is a fundamental climatological variable, especially in areas where waste is being dumped, since the volumes of precipitated water represent the main input of water into the water balance of an area, contributing to the increase in leachate. It is also worth noting that precipitation has adverse effects when intense events occur and are amplified by anthropogenic factors, such as floods and inundations. In urban solid waste dumps, precipitation can cause problems beyond the increase in leachate, such as, for example, the rise in water levels of rivers and streams, leading to flooding problems in the area.

In addition to the magnitude of precipitation, it is essential to understand the recurrence times of precipitation (MELLO et al., 2001). The recurrence times or return periods of intense precipitation can be obtained from estimates, based on mathematical probability distribution models, which use statistical inference to estimate the parameters of the structures of these models (NAGHETTIN and PINTO, 2007). In such studies, continuous probability distributions are widely used. For series of maximum daily precipitation values, the Gumbel distribution is one of the most used in several studies (ABUBAKARI, KUSI and XIAOHUA, 2017, OLIVEIRA JÚNIOR, et al., 2019).

From the heavy rainfall associated with the times of recurrence, it is possible to assess the increase in the level of water bodies in a region and map the water spots, thus enabling the verification of the areas that may be affected by flooding. Silva et al. (2023) mention some problems caused by the incidence of heavy rainfall in a region, such as: soil erosion, destruction of crops, occurrence of floods, inundations and flooding, intensification of the silting process, and rupture of dams.

In this sense, it is important to carry out studies that characterize the degraded area of deactivated landfills before determining the recovery techniques. After all, knowledge of the area makes it possible to determine the techniques that will be truly efficient in the recovery process of these areas (REZENDE et al., 2013).

Therefore, the objective of the present work is to evaluate historical precipitation series from pluviometric stations located close to the Lixão do Roger area in João Pessoa-PB, estimate maximum precipitation using continuous probability distribution (Gumbel) for different recurrence times, and map the floods generated by these precipitations associated with the recurrence times studied, guaranteeing the safety of the redeveloped area.

2. Methodology

The Lixão do Roger area is located in the municipality of João Pessoa, in the Paraíba River basin, and is located at geographic coordinates 7°6'18.89"S and 34°53'5.08"W, altitude of 15 m. In hydrological terms, the study area is located in the lower reaches of the Paraíba River, drained by a tributary of the Sanhauá River. Figure 1 shows a location diagram of the study area.

Rainfall data made available on the National Water and Basic Sanitation Agency (ANA, 2022) website were used to characterize rainfall in the study area. The data can be downloaded from the Hidroweb v.3.2.6 website.

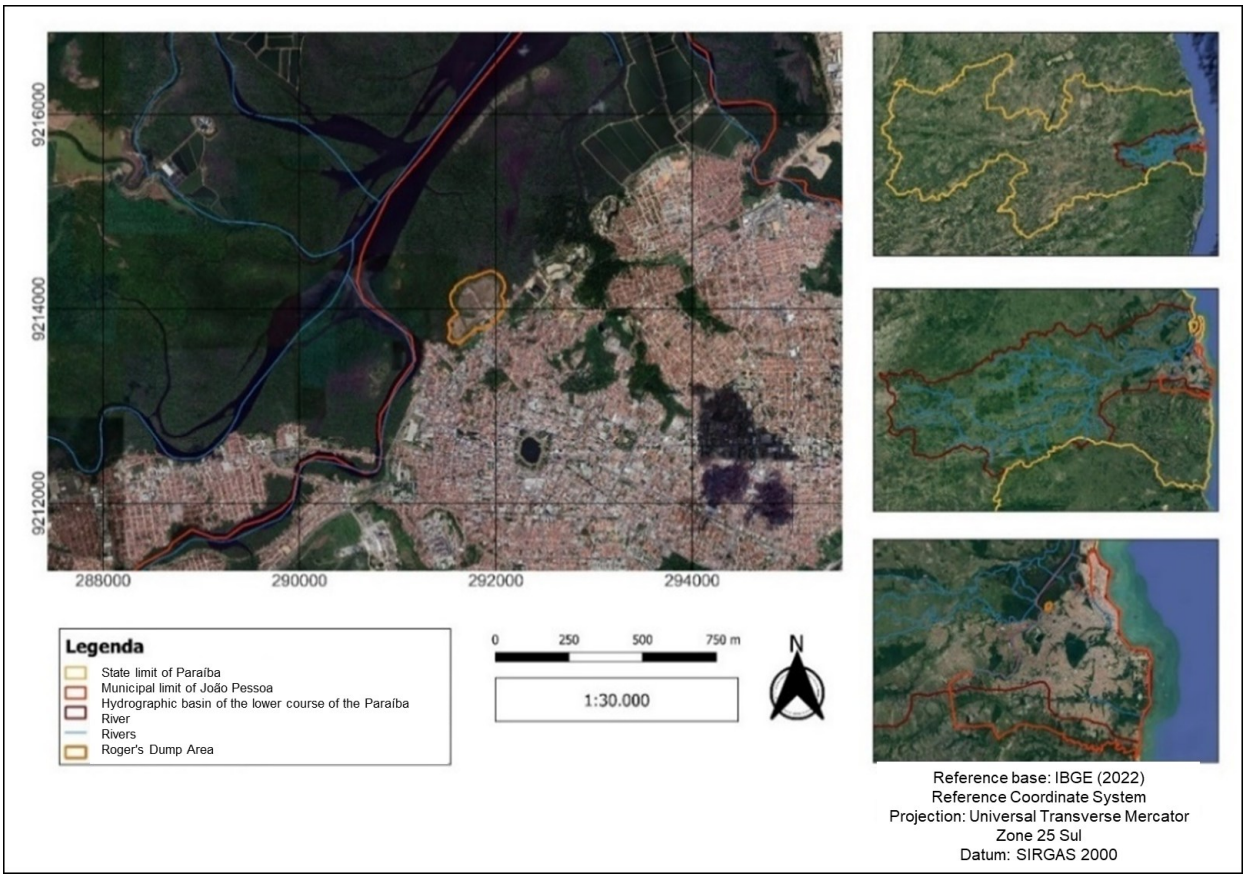

Figure 1 – Location of the study area.
Source: Authors (2024).

The characterization was carried out from the CAGEPA Station located in Cabedelo (Station Code 734042), the INMET Station located in João Pessoa (Station Code 734006), and the Cemaden Station located in Bayeux (Station Code 734044) specialized in the Area's contribution basin of Lixão do Roger, as shown in Figure 2.

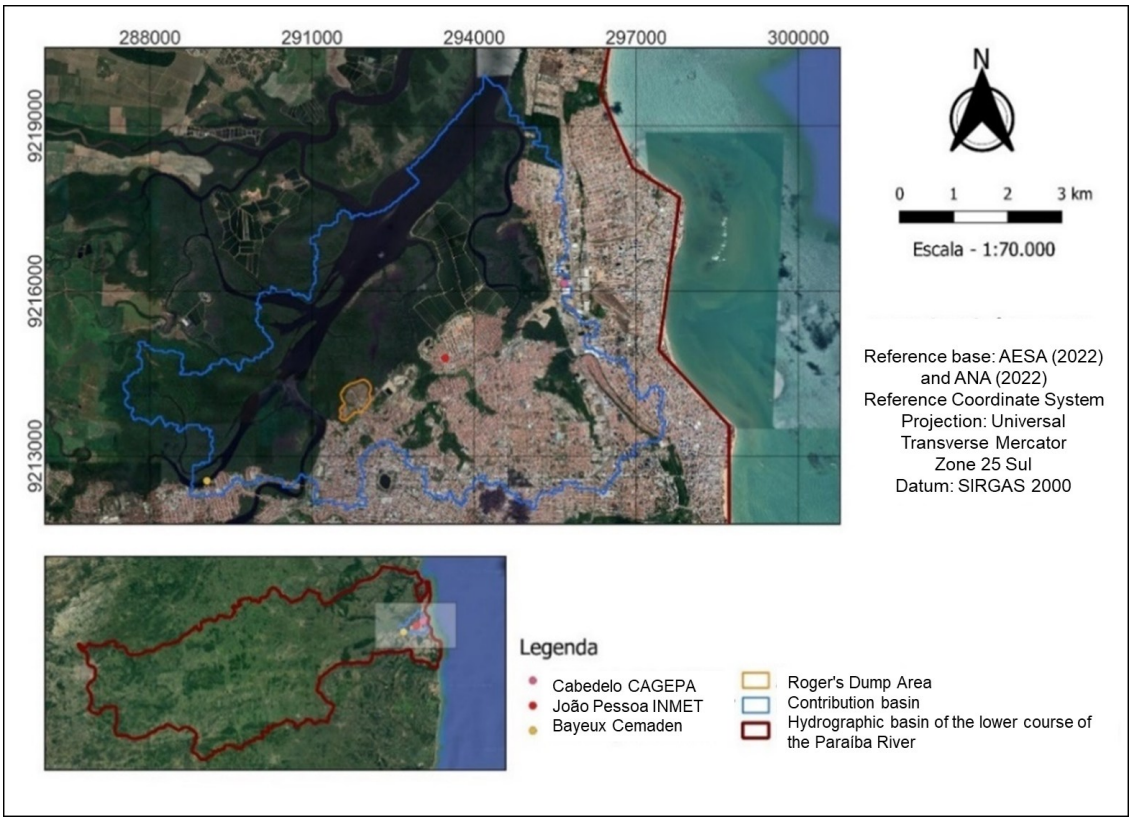

Figure 2 – Location in the contribution basin of the Rain Gauge Stations used to characterize precipitation. Source: Authors (2024).

The rainfall data series were analyzed, and the series with missing data, which was more significant than 10%, were discarded, following the criteria of Aryee et al. (2018). The absolute and relative homogeneity of the rainfall data was also verified, according to Alexandersson and Moberg (1997). For this reason, a historical series of 18 years was used, from January 2002 to December 2019, considering that this period presented the fewest failures and the most excellent homogeneity of data among the three stations. To analyze the consistency of the data, the double mass method was used to compare the annual accumulated values of each station with the accumulated values of a neighboring reference station.

The probabilistic method used was the Gumbel distribution, and the maximum rainfall was calculated for the recurrence times of 2, 5, 10, 25, 50, and 100 years.

The Gumbel distribution was selected because it suits a historical series of maximum extreme values (NAGHETTINI and PINTO, 2007). Its parameters were estimated using the method of moments. The Gumbel method is based on the following Cumulative Probability Function, given by:

$$P = 1 - e^{-e^{-yi}} \tag{1}$$

Where P is the probability of any of the maxima being equaled or exceeded, and yi is the reduced variable given by:

$$yi = a(Xi - Xf) \tag{2}$$

Where yi is the reduced variable of the i maximum recorded precipitations, Xi is the maximum recorded precipitations, and the parameters a and Xf are given by:

$$a = \frac{Sn}{Sx} \tag{3}$$

$$Xf = \overline{X} - Sx\left(\frac{\overline{Y}n}{Sn}\right) \quad (4)$$

Where $\overline{X}$ is the mean of the maximum recorded precipitation, Sx is the standard deviation of the maximum recorded precipitation. The $\overline{Y}n$ e Sn are values associated with the reduced variable and tabulated according to the number of data made available in Vilela (1975), as shown in Table 1.

After calculating all parameters, they were applied to equation 2, thus obtaining the corresponding values of the reduced variables for each maximum recorded precipitation. A graph of reduced variables versus maximum recorded precipitation was then plotted. A linear regression equation was estimated using this graph. This equation was later used to calculate the maximum precipitation associated with the return periods. Table 2 shows the corresponding reduced variables for different return periods.

Table 1 – Expected values of the mean (Yn) and standard deviation (Sn) of the reduced variable (y) as a function of the number of data (n).

n	$\overline{Y}n$	Sn	n	$\overline{Y}n$	Sn
10	0.49	0.95	80	0,56	1,19
20	0.52	1.06	90	0,56	1,20
30	0.54	1.11	100	0,56	1,21
40	0.54	1.14	150	0,56	1,23
50	0.55	1.16	200	0,57	1,24
60	0.55	1.17	∞	0,57	1,28
70	0.55	1.19	-	-	-

Source: Vilela (1975).

Table 2 – Reduced variable and return period.

Reduced Variable (y)	Return Period (Tr)
0.000	1,58
0.367	2
0.579	2,33
1.500	5
2.250	10
2.970	20
3.182	25
3.395	30
3.902	50
4.600	100
5.296	200
5.808	300
6.214	500
6.907	1000

Source: Vilela (1975).

The HMS (Hydrologic Engineering Center - Hydrologic Modeling System) software was used to estimate the flows generated by rainfall associated with the recurrence times. The contribution area was calculated using the cartographic base of the Executive Agency for Water Management (AESA) of Paraíba and data from the Shuttle Radar Topography Mission (SRTM).

The alternating block method was used to construct the hyetograph. The Curve Number (CN) method, developed by the Natural Resources Conservation Service (NRCS), was used to determine the adequate precipitation.

The CN value accounts for most of the characteristics of the runoff-producing river basins, such as soil type, land use, hydrological condition, and previous moisture condition (MISHRA & SINGH, 2004). To estimate the adequate precipitation, Equation 5 was applied:

$$\mathrm{Pe} = \frac{(P-Ia)^2}{P-Ia+S} \quad (5)$$

For P> Ia e 0 in other cases

Where Pe is the adequate rainfall in mm, P is total precipitation in mm, Ia is the initial abstraction in mm, and S is the maximum soil retention potential in mm.

For Ia, the value of 0.2S was adopted, as recommended by the NRCS. Thus, equation 5 can be rewritten in the form of Equation 6:

$$\mathrm{Pe} = \frac{(P-0{,}2S)^2}{P+0{,}8S} \quad (6)$$

Where S is obtained by equation 7:

$$\mathrm{S} = \frac{25400}{CN} - 254 \quad (7)$$

The CN parameter is related to the soil type, the type of vegetation cover and the antecedent moisture conditions. In this study, the antecedent condition of average moisture was considered for a type B soil with vegetation cover type: urban, vegetated area and riparian forest. In the CN estimation, aerial images of the municipality were used, combined with images from Google Earth. It is worth noting that the value of the CN number was estimated from the values in the table determined by the NRCS, according to the soil type of the study area. To obtain the flood hydrograph from the rainfall hyetograph, the NRCS Dimensionless Unit Hydrograph method was applied, following the proposal of Ebrahimian et al., (2012). The method has as a parameter the delay time (Tlag). The Tlag value is obtained by equation 8:

$$\mathrm{Tlag} = 0{,}6 * \mathrm{Tc} \quad (8)$$

Where Tc is the concentration time in minutes and Tlag is the delay time in minutes.

The concentration time can be estimated by equation 9:

$$\mathrm{Tc} = 3{,}98\ \frac{L^{0,77}}{D^{0,385}} \quad (9)$$

Where Tc is the time of concentration in minutes, L is the length of the river in km and D is the slope in %.

The maximum flows obtained in the hydrological modeling for rainfall at recurrence times of 2, 5, 10, 25, 50, and 100 years, as well as the hydraulic elements (drainage network, cross-sections, and channel limits), were entered as input data in the HEC-RAS model.

The permanent flow regime was adopted due to the limitation of data on an hourly scale. Thus, the value obtained refers to the flooded area at the maximum flood caused by the rainfall event simulated in the study.

The Manning roughness coefficient (n) value was selected using georeferenced Google Earth images dated December 12, 2018. For flow in the river channel, n = 0.08 was adopted as the initial value, and for flow in the floodplain, on both banks, n = 0.12 was taken.

Using the RAS mapper tool of HEC-RAS and HEC-HMS, it was possible to prepare the data set required for the hydraulic simulation. The main channel was delimited to distinguish the main channel from the floodplains, thus defining the smaller bed of each watercourse.

The shaded terrain model obtained from the DEM was used to guide the delimitation of this element. In this way, it was possible to visually identify the topographic details of the river channels of interest. The Flow Lines of each watercourse were delimited considering the flow in the channel thalweg and the flow over the larger bed along the banks. They consisted of lines indicating the direction of flow in these locations.

The cross sections were the main elements for the hydraulic simulation since the elevation levels from the DEM were extracted from them to generate the profiles in each section of the channel and compute the hydrological input information for the subsequent simulation in the HEC-RAS software.

After calculating the water surface profiles, the results were exported to shapefile format. The water levels in each section were overlaid on the Shuttle Radar Topography Mission (SRTM) to estimate the flooding areas. The data used in the modeling are described in Table 3.

Table 3 – Hydrological modeling parameters.

Area (km²)	38.26
L (km)	8.79
Unevenness (%)	0.3
CN	75
Tc (min.)	33.73
S (mm)	84.67

Source: Authors (2024).

3. Results and discussions

The annual precipitation of the 18-year historical series (2002 to 2019) obtained at Posto Cabedelo (CAGEPA) corresponded on average to approximately 1,698.8 mm and a coefficient of variation of 24.9%. This indicates that the series of data of average annual precipitation of the 18 years presents low dispersion. The most significant precipitation occurred in June, an average of 366.3 mm, representing approximately 21.6% of all the average annual precipitation. This was the month with the lowest coefficient of variation, approximately 42.8%, indicating that June had the most homogeneous behavior about the dispersion of precipitation throughout the months. On the other hand, the month with the lowest average precipitation is the month of November, approximately 14.5 mm, representing approximately 0.86% of the total annual precipitation. Regarding the coefficient of variation, December, followed by November, had the highest percentage, approximately 103.6%, and 94.8%, respectively. These results indicate that the periods of November and December are the most heterogeneous in the dispersion of precipitation throughout the months.

At Posto Cabedelo Cagepa, the annual precipitation of the 18-year historical series (2002 to 2019) corresponded on average to approximately 1,698.8 mm and a coefficient of variation of 24.9%. This indicates that the series of data on average annual precipitation of the 18 years has low dispersion. The highest precipitation occurred in June, an average of 366.3 mm, representing approximately 21.6% of all the average annual precipitation. This month had the lowest coefficient of variation, approximately 42.8%, indicating that June is the one with the most homogeneous behavior about the dispersion of precipitation throughout the months.

Figure 3 shows the fluctuations in annual precipitation in the historical series analyzed at Posto Cabedelo Cagepa. Generally, there are years above and below the average without any apparent trend. Another important aspect is the occurrence of precipitation above and below the standard deviation plus the average and the standard deviation minus the average. This suggests conditions of extreme precipitation in larger and smaller amounts than usual observed in the region. This behavior may be associated with global changes that cause changes in the rainfall regime, which may result in larger and smaller volumes than expected for a given region. Using the criterion of Almeida and Porto (2021), it can be noted that 66.67% of the years in the historical series presented annual precipitation values between the average ± standard deviation, indicating that the observed variability may present some level of anthropogenic intervention.

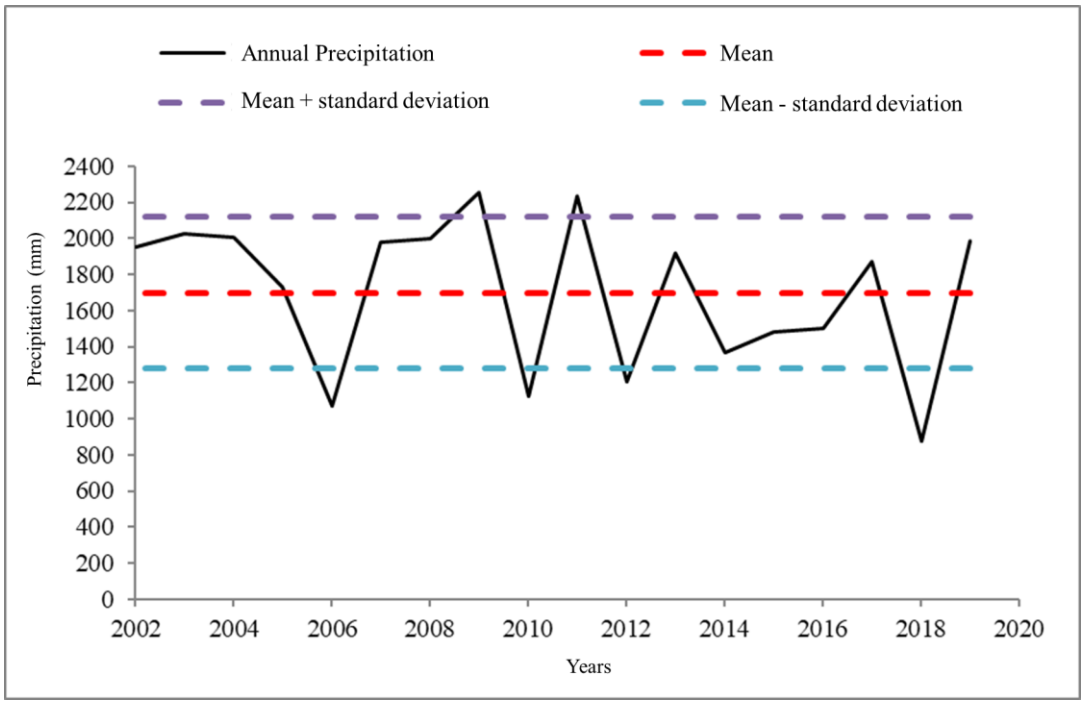

Figure 3 – Precipitation fluctuation over the years and statistical analysis of Posto Cabedelo Cagepa. Source: Authors (2024).

On the other hand, the annual precipitation of the 17-year historical series (2002 to 2018) obtained from the João Pessoa INMET Station presented an average of 1,875.1 mm and a coefficient of variation of 20.7%. This indicates that the data series on average annual precipitation of the 17 years presents low dispersion, similar to the Cabedelo Cagepa Station. At the João Pessoa INMET Station, the highest precipitation occurs in June, an average of 400.3 mm, representing approximately 21.3% of the total annual average precipitation. This was the month with the lowest coefficient of variation, approximately 41.7%, indicating that June is also the one with the most homogeneous behavior about the dispersion of precipitation throughout the months at the João Pessoa INMET Station.

November also has the lowest average precipitation at the João Pessoa INMET Station, approximately 18.3 mm, representing approximately 0.97% of the total annual precipitation. Regarding the coefficient of variation, November had the highest percentage, approximately 88.3%. This result indicates that November is the most heterogeneous month in terms of the dispersion of the amount of precipitation over the months.

Figure 4 shows the fluctuations in annual precipitation in the historical series analyzed at the João Pessoa INMET Station. It is possible to see that, in general, there are also years above and below the average without any apparent trend similar to that observed at the Cabedelo Cagepa Station. The same aspect of precipitation occurring above and below the standard deviation plus the average and the standard deviation minus the average is also observed at the João Pessoa INMET Station. Using the criterion of Almeida and Porto (2021), it is noted that 77.78% of the years in the historical series presented annual precipitation values between the average ± standard deviation, indicating that the observed variability may present some level of anthropic intervention.

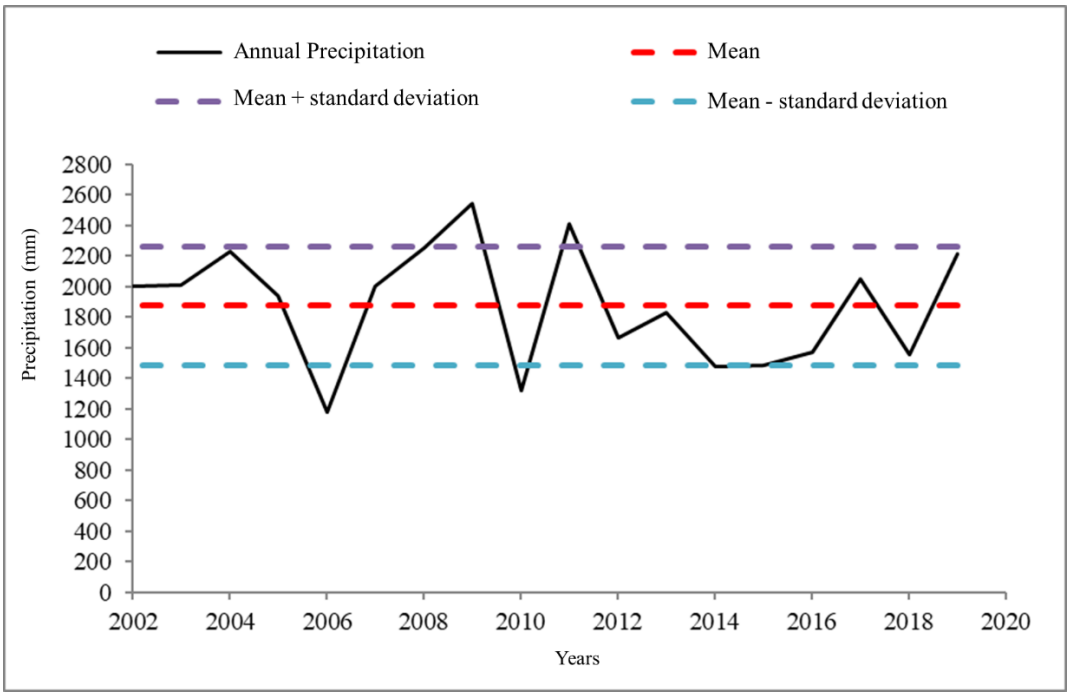

Figure 4 – Precipitation fluctuation over the years and statistical analysis of the João Pessoa INMET Station. Source: Authors (2024).

At the Bayeux Cemaden Station, the annual precipitation of the 18-year historical series (2002 to 2019) averaged 1,839.3 mm and had a coefficient of variation of 19.8%. This indicates that the data on the average annual precipitation of the 18 years have low dispersion, similar to the other series of the stations analyzed.

At the Bayeux Cemaden Station, the highest average precipitation also occurs in June, on average 383.3 mm, representing approximately 20.84% of all the average annual precipitation. This was the month with the lowest coefficient of variation, approximately 47.4%. This indicates that June is also the one with the most homogeneous behavior about the dispersion of precipitation throughout the months, similar to the other stations.

The month with the lowest average precipitation at Posto Bayeux Cabedelo is November, approximately 16.7 mm, representing approximately 0.91% of the total annual precipitation. Regarding the coefficient of variation, December, followed by November, was the month with the highest percentage, approximately 99.7% and 99.5%, respectively. These results indicate that the period of November and December is the most heterogeneous in the dispersion of precipitation throughout the months, similar to the behavior observed at Posto Cabedelo Cagepa. Figure 5 shows the oscillations of the annual precipitation of the historical series analyzed at Posto Bayeux Cemaden.

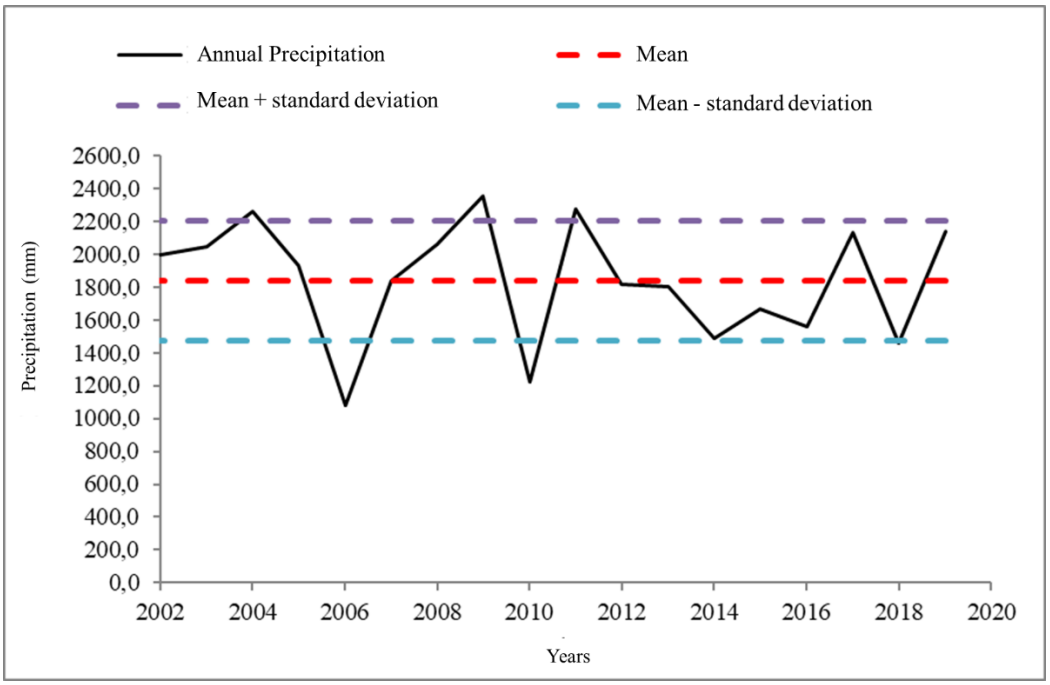

Figure 5 – Precipitation fluctuation over the years and statistical analysis of the Bayeux Cemaden Station. Source: Authors (2024).

It is possible to verify that, in general, there are also years above and below the average without any apparent trend similar to the other stations. The same aspect of precipitation occurring above and below the standard deviation plus the average and the standard deviation minus the average is also observed at the Bayeux Cemaden Station. Using the criterion of Almeida and Porto (2021), it is noted that 72.22% of the years in the historical series presented annual precipitation values between the average ± standard deviation, indicating that the observed variability may present some level of anthropic interventions.

When evaluating the three stations, it is possible to identify that they all behave similarly at a monthly and annual level and in terms of sensitivity to climate change.

Based on the historical series of annual maximum daily precipitation at the Cabedelo Cagepa station, the class with the highest frequency of occurrence was class 3, with precipitation between 114.58 mm and 146.02 mm (Table 4). It is observed that the values of these classes present precipitations greater than the average maximum annual precipitation of 113.5 mm in the period evaluated at Posto Cabedelo Cagepa.

Table 4 – Frequency distribution of maximum rainfall at Posto Cabedelo Cagepa.

Class	Class intervals	Observed frequency
1	51.70 - 83.14	3
2	83.14 - 114.58	6
3	114.58 - 146.02	7
4	146.02 - 177.46	1
5	177.46 - 208.9	1

Source: Authors (2024).

At the João Pessoa INMET Station, the historical series of maximum daily annual precipitation, the class that presents the highest frequency of occurrence are classes 2 and 3, with precipitation between 83.83 mm and 116.66 mm in class 2 and precipitation between 116.66 mm and 149.49 mm in class 3 (Table 6). It is observed that the values of these classes present lower precipitation (class 2) and higher (class 4) than the average maximum annual precipitation of 122.3 mm in the period evaluated at the João Pessoa INMET Station.

Table 5 – Frequency distribution of maximum rainfall at João Pessoa INMET Station.

Class	Class intervals	Observed frequency
1	51.00 - 83.83	2
2	83.83 - 116.66	6
3	116.66 - 149.49	6
4	149.49- 182.32	3
5	182.32 - 215.15	1

Source: Authors (2024).

At the Bayeux Cemaden Station, the historical series of maximum daily annual precipitation shows that the class with the highest occurrence frequency is class 2, with precipitation between 84.90 mm and 118.40 mm (Table 6). It can be seen that the values of these classes present precipitation lower than the average maximum annual precipitation of 122.15 mm in the period evaluated at the Bayeux Cemaden Station.

Table 6 – Frequency distribution of maximum rainfall at Bayeux Cemaden Station.

Class	Class intervals	Observed frequency
1	51.40 - 84.90	3
2	84.90 - 118.40	6
3	118.40 - 151.90	5
4	151.90 - 185.40	3
5	185.40 - 218.9	1

Source: Authors (2024).

Some studies carried out in the Northeast region of Brazil, such as Oliveira Júnior et al. (2019) and Silva et al. (2023), using the same methodology, found higher frequencies of maximum rainfall in classes 3 and 4, with intervals ranging from 79.47 mm to 95.98 mm in the municipality of Crato, Ceará, and with intervals ranging from 82.20 mm to 99.10 mm in the municipality of Serra Talhada. These values quantitatively demonstrate the more significant rainfall input on the coast about the more continental areas of the region. This behavior reinforces the importance of understanding the impacts of rainfall on the urban space of coastal cities, especially the capitals, where human interventions may be more significant due to the size of the cities.

The means, standard deviation, and parameters of the Gumbel distribution of Posto Cabedelo Cagepa's maximum rainfall series were calculated, as shown in Table 7 and Figure 6. Calculated.

Table 7 – Values used and calculated for applying the Gumbel distribution to the Cabedelo Cagepa Station.

Parameter	Value	Source
Mean	113.52	Calculated
Standard deviation	33.91	Calculated
Yn	0.51	Interpolated by Table 2
Sn	1.04	Interpolated by Table 2
Xf	96.73	Calculated by Equation 4
a	0.03	Calculated by Equation 3

Source: Authors (2024).

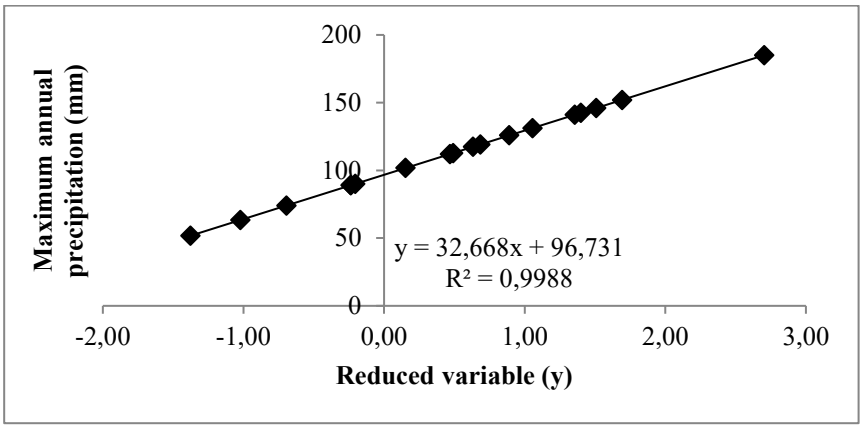

Figure 6 – Graph of reduced variable versus maximum annual precipitation recorded at Posto Cabedelo Cagepa. Source: Authors (2024).

The results of determining the maximum rainfall associated with the different return periods obtained by the Gumbel distributions from the equation obtained graphically in Figure 6 are presented in Table 8 for Posto Cabedelo - Cagepa.

Table 8 – Maximum precipitation and its respective return periods for Posto Cabedelo Cagepa.

	Gumbel Method	
Return period Tr (years)	**Reduced variable y**	**Maximum Precipitation P (mm)**
2	0.367	108.72
5	1.5	145.73
10	2.25	170.23
25	3.2	201.27
50	3.9	224.14
100	4.6	247.00

Source: Authors (2024).

The averages, standard deviations, and parameters of the Gumbel distribution of the maximum precipitation series of the João Pessoa INMET Station were calculated, as shown in Table 9 and Figure 7.

Table 9 – Values used and calculated for applying the Gumbel distribution to the João Pessoa INMET Station.

Parameter	Value	Source
Mean	122.26	Calculated
Standard deviation	35.73	Calculated
Yn	0.51	Interpolated by Table 2
Sn	1.04	Interpolated by Table 2
Xf	104.56	Calculated by Equation 4
a	0.03	Calculated by Equation 3

Source: Authors (2024).

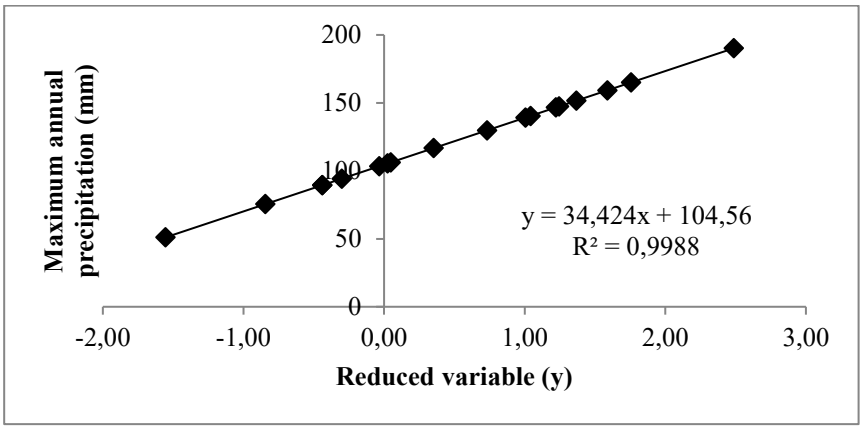

Figure 7 – Graph of reduced variable versus maximum annual precipitation recorded at the João Pessoa INMET Station. Source: Authors (2024).

Table 10 presents the results of determining the maximum rainfall associated with the different return periods obtained by the Gumbel distributions from the equation obtained graphically in Figure 7 for the João Pessoa—INMET Station.

Table 10 – Maximum precipitation and their respective return periods for the João Pessoa INMET Station.

	Gumbel Method	
Return period Tr (years)	**Reduced variable y**	**Maximum Precipitation P (mm)**
2	0.367	117.19
5	1.5	156.20
10	2.25	182.01
25	3.2	214.72
50	3.9	238.81
100	4.6	262.91

Source: Authors (2024).

The means, standard deviations, and parameters of the Gumbel distribution of the maximum precipitation series of the Bayeux Cemaden Station were calculated, as shown in Table 11 and Figure 8.

Table 11 – Values used and calculated for applying the Gumbel distribution to the Bayeux-Cemaden Station.

Parameter	Value	Source
Mean	122.15	Calculated
Standard deviation	38.82	Calculated
Yn	0.51	Interpolated by Table 2
Sn	1.04	Interpolated by Table 2
Xf	102.92	Calculated by Equation 4
a	0.03	Calculated by Equation 3

Source: Authors (2024).

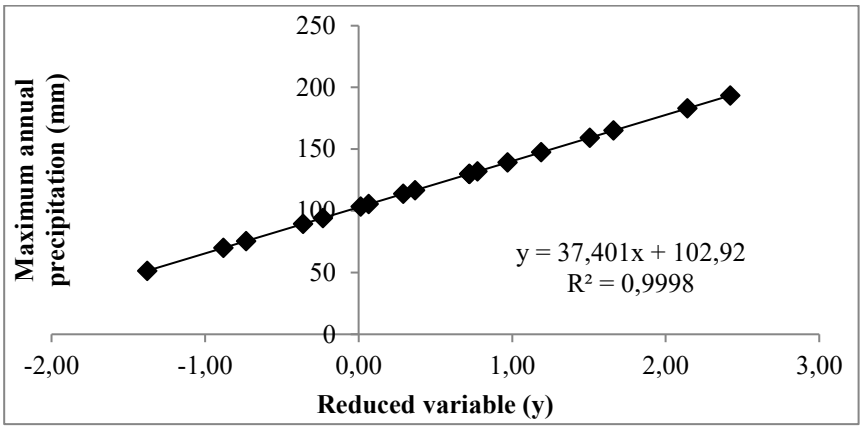

Figure 8 – Graph of reduced variable versus maximum annual precipitation recorded at Bayeux-Cemaden Station. Source: Authors (2024).

The results of determining the maximum rainfall associated with the different return periods obtained by the Gumbel distributions from the equation obtained graphically in Figure 8 are presented in Table 12 for the Bayeux-Cemaden Station.

Table 12 – Maximum precipitation and their respective return periods for the Bayeux - Cemaden Station.

	Gumbel Method	
Return period	**Reduced variable**	**Maximum Precipitation**
Tr (years)	**Y**	**P (mm)**
2	0.367	116.65
5	1.5	159.02
10	2.25	187.07
25	3.2	222.60
50	3.9	248.78
100	4.6	274.96

Source: Authors (2024).

The results of the flows associated with the recurrence times obtained with the hydrological modeling of the Cabedelo Cagepa Station, João INMET Station and Bayeux Cemaden Station are presented respectively in Tables 13, 14 and 15.

Table 13 – Maximum flow rates obtained for the Cabedelo Cagepa Station

Tr (years)	Maximum Precipitation (mm)	Maximum Flow Rates (m³/s)	Flood Altimetric Level (m)
2	108.72	171.97	2.13
5	145.73	524.89	4.10
10	170.23	613.14	4.57
25	201.27	724.94	5.14
50	224.14	807.31	5.55
100	247	889.65	5.87

Source: Authors (2024).

Table 14 – Maximum flow rates obtained for the João Pessoa INMET Station.

Tr (years)	Maximum Precipitation (mm)	Maximum Flow Rates (m³/s)	Flood Altimetric Level (m)
2	117.19	195.78	2.27
5	156.2	311.96	2.94

10	182.01	393.01	3.39
25	214.72	498.85	3.96
50	238.81	578.44	4.39
100	262.91	659.10	4.80

Source: Authors (2024).

Table 15 – Maximum flow rates obtained for the Bayeux Station.

Tr (years)	Maximum Precipitation (mm)	Maximum Flow Rates (m³/s)	Flood Altimetric Level (m)
2	116.65	194.24	2.26
5	159.02	320.68	2.99
10	187.07	409.18	3.48
25	222.6	524.75	4.10
50	248.78	611.69	4.56
100	274.96	699.76	5.01

Source: Authors (2024).

Figure 9 shows the flooded areas for the return time of 2, 5, 10, 25, 50, and 100 years obtained with the precipitation series of the Cabedelo Cagepa Post. Table 16 shows the areas calculated for each flood spot and those subject to flooding within the limits of the Roger landfill. It can be observed that flooding that reaches the Roger landfill's limits can occur for rains with a recurrence time of 25 years or more. The flood spot for Tr = 25 years intercepts the northeast portion of the limits of the Roger landfill. For Tr = 50 and 100 years, the spots, in addition to intercepting the northeast portion, also intercept the southeast, south, and southwest portions. The northern portion was the only one not intercepted by the flooded spot, even for Tr = 100 years.

Table 16 – Calculated areas of flood spots and areas liable to flooding in the Roger do Posto Cabedelo Cagepa landfill.

Tr (years)	Flooded Area (km²)	Flooded Area (%)	Area liable to flooding of Lixão do Roger (km²)	Area liable to flooding of Lixão do Roger (%)
2	6.60	17.25	0	0
5	7.50	19.59	0	0
10	7.85	20.53	0	0
25	9.92	25.93	0.04	12.07
50	12.57	32.86	0.07	22.76
100	14.263	37.28	0.09	30.00

Source: Authors (2024).

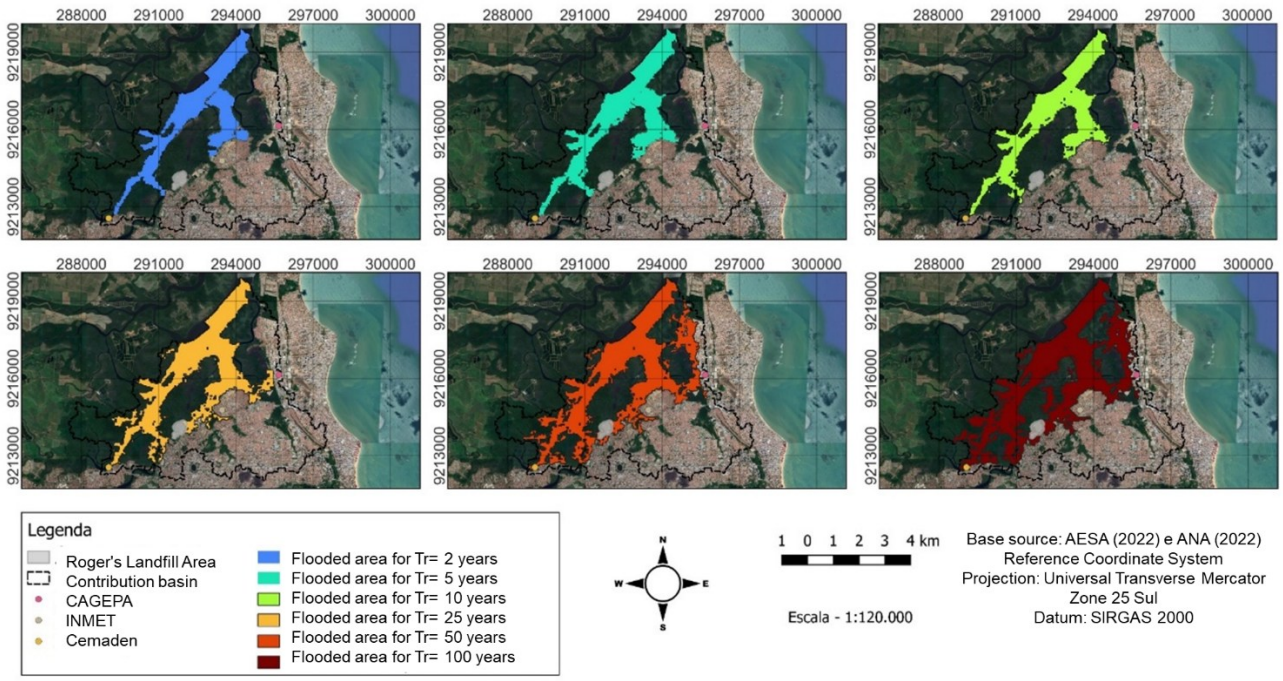

Figure 9 – Delimitation map of flooded areas for different recurrence times based on data from Posto Cabedelo Cagepa. Source: Authors (2024).

Figure 10 shows the flooded areas for the return time of 2, 5, 10, 25, 50, and 100 years obtained with the precipitation series from the João Pessoa INMET Station. Table 17 shows the areas calculated for each flood spot and the areas subject to flooding within the limits of the Roger landfill. It can be seen that the flood spots are not intercepted, not even for floods of Tr = 100 years.

Table 17 – Calculated areas of flood spots and areas liable to flooding at the Roger landfill at Posto João Pessoa INMET.

Tr (years)	Flooded Area (km²)	Flooded Area (%)	Area liable to flooding of Lixão do Roger (km²)	Area liable to flooding of Lixão do Roger (%)
2	6.66	17.41	0.00	0.00
5	6.89	18.02	0.00	0.00
10	7.11	18.59	0.00	0.00
25	7.43	19.42	0.00	0.00
50	7.70	20.13	0.00	0.00
100	7.98	20.87	0.00	0.00

Source: Authors (2024).

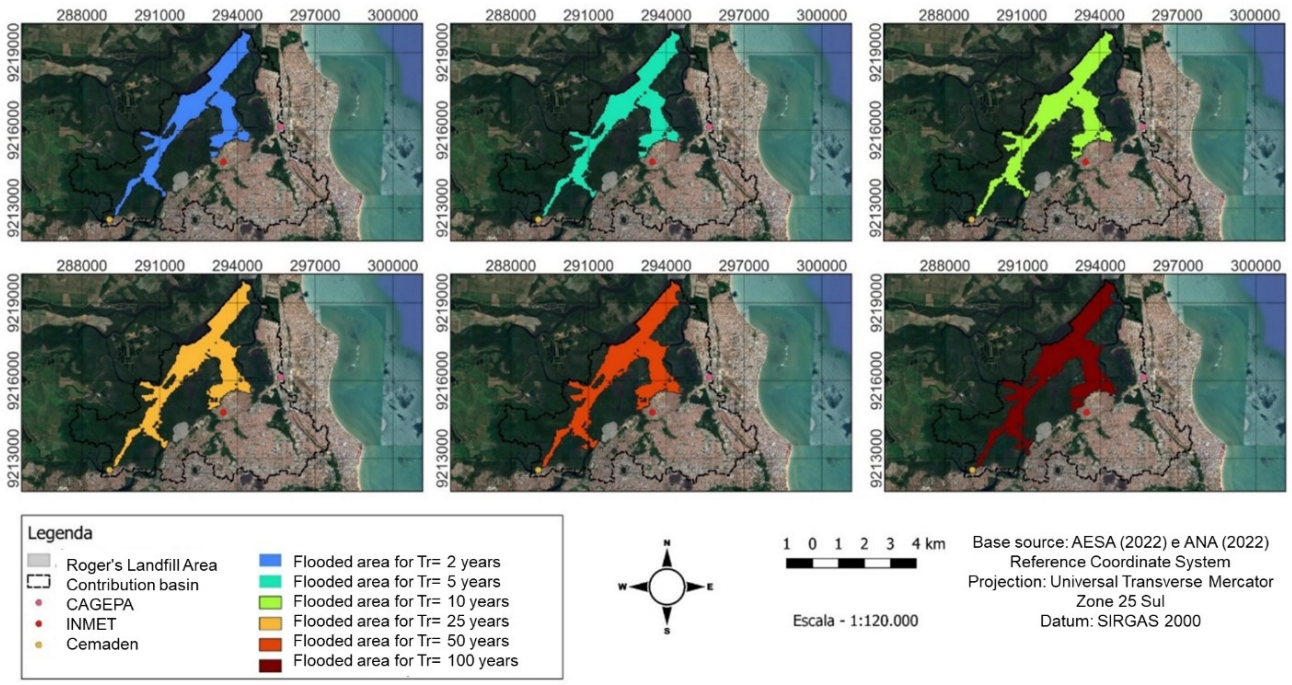

Figure 10 – Delimitation map of flooded areas for different recurrence times based on data from the João Pessoa INMET Station.
Source: Authors (2024).

Finally, Figure 11 shows the flooded areas for the return time of 2, 5, 10, 25, 50 and 100 years obtained with the precipitation series from the Bayeux Cemaden Station. Table 18 shows the areas calculated for each flood spot and the areas subject to flooding within the limits of the Roger landfill. It can be seen that only the flood spot of Tr = 100 years intersects the limits of the Roger landfill. The flood spot is observed in the northeast, east and southeast portions of the Roger landfill area.

Table 18 – Calculated areas of flood spots and areas liable to flooding at Lixão do Roger do Posto Bayeux Cemaden.

Tr (years)	Flooded Area (km²)	Flooded Area (%)	Area liable to flooding of Lixão do Roger (km²)	Area liable to flooding of Lixão do Roger (%)
2	6.64	17.36	0.00	0.00
5	6.94	18.13	0.00	0.00
10	7.16	18.71	0.00	0.00
25	7.50	19.59	0.00	0.00
50	7.84	20.49	0.00	0.00
100	9.27	24.22	0.03	11.72

Source: Authors (2024).

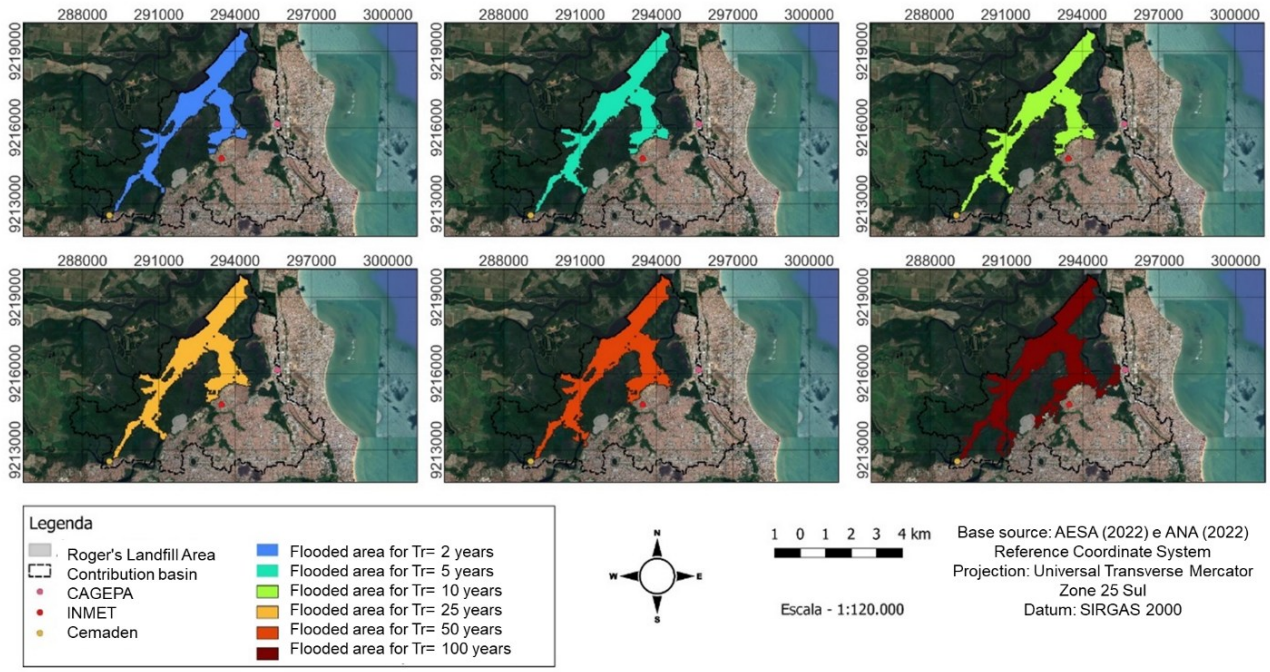

Figure 11 – Delimitation map of flooded areas for different recurrence times based on data from the Bayeux Cemaden Station.
Source: Authors (2024).

As reported by Monte et al. (2016), hydrological modeling provides a good capacity to represent flood events in the geographic space under analysis. This behavior was also observed in the analysis presented in the present study.

4. Final considerations

The methodology used allowed for the simulation of flooding scenarios caused by rising water levels in rivers near the Roger landfill in João Pessoa. This enabled the satisfactorily achieved identification of areas affected by flooding and the elevations reached for different rainfall recurrence times.

The rainfall stations show similar behavior, with the highest rainfall volumes occurring in the first half of the year, with peak rainfall in May and June. The total annual rainfall from the statistical analyses shows occurrences of values that may be associated with the effects of climate change.

The maximum rainfall associated with the recurrence times was adequate in hydrological modeling. It demonstrated that floods with recurrence times of 25 to 100 years may affect the Roger landfill area. The Roger landfill area may be more affected by the maximum rainfall occurring in the regions of the Cabedelo Cagepa and Bayeux Cemaden stations, possibly because they are located on the edges of the studied concentration basin, and neighboring hydrological regions influence precipitation volumes.

Based on the hydrological modeling and the delimitation of the flood areas in the Roger Landfill area, it can be seen that the highest altimetric elevation that the flood spots reached was approximately 5.87 m (Tr = 100 years of the Cabedelo Cagepa Post). Therefore, construction of electrical, hydraulic, telecommunications, etc. infrastructures is not recommended to be carried out below the altimetric elevation of 6 m due to the high risk of these areas being hit by floods from maximum secular rainfall.

It is worth noting that in the regions intercepted by the flood spots, containment measures that can reduce or eliminate the physical effect of the flood wave of the contributing basin are suggested to protect the areas on the edges of the Roger Landfill area, especially in the northeast, east, and southeast portions, which are the limits of the land most affected by the flood spots in the study carried out.

Acknowledgements

The authors would like to thank the city of João Pessoa and the Sustainable João Pessoa Program Consórcio Terra & Promon, which aimed to develop studies and projects for the environmental recovery of Lixão do Roger and the preparation of projects for the creation of the Socio-Environmental Park.

References

Abubakari. S.; Kusi. K. A.; Xiaohua. D. Revision of the Rainfall Intensity Duration Frequency Curves for the City of Kumasi-Ghana. *The International Journal Of Engineering And Science*. v.6. n.1. p.51-56. 2017.

Almeida. H. A.; Porto. J. C.G. Temporal oscillations in the rain regime in Curimatáu paraibano: variability. extreme or climate change? Journal of Hyperspectral Remote Sensing. v.11. n.5. p. 262-270. 2021.

ANA. *Agência Nacional de Águas e Saneamento Básico*. Disponível em: https://www.snirh.gov.br/hidroweb/apresentacao. Acesso em: 27 de outubro de 2023.

Alexandersson. H.; Moberg. A. Homogenization of Swedish temperature data. Part I: Homogeneity test for linear trends. *International Journal of Climatology*. v.17. p. 25–34. 1997.

Aryee. J. N. A.. Amekudzi. L. K.. Quansah. E.. Klutse. N. A. B.. Atiah. W. A.. & Yorke. C. Development of high spatial resolution rainfall data for Ghana. *International Journal of Climatology*. v.38. n.3. p. 1201–1215. 2018.

Ebrahimian. M.; Nuruddin. A.A.; Soom. M.A.B.M.; Sood. A.M. Application of NRCS-curve number method for runoff estimation in a mountainous watershed. *Journal of Environmental Sciences*. v.10. p. 103-114. 2012.

Lisboa. F. M.; Donagemma. G. K.; Burak. D. L.; Passos. R. R.; Mendonça. E. S. Indicadores de qualidade de Latossolo relacionados à degradação de pastagens. *Pesquisa agropecuária brasileiro*. V.51. n.9. p.1184-1193. 2016.

Mello. C. R.; Ferreira. D. F.; Silva. A. M.; Lima. J. M. Análise de modelos matemáticos aplicados ao estudo de chuvas intensas. *Revista Brasileira de Ciência do Solo*. v.25. n.3. p.693-698. 2001.

Monte. B. E.O.; Costa. D. D.; Chaves. M. B.; Magalhães. L. de O.; Uvo. C. B. Modelagem Hidrológica e hidráulica aplicada ao mapeamento de áreas inundáveis. *Revista Brasileira de Recursos Hídricos*. v. 21. n. 1. p. 152-167. 2016.

Naghettini. M.; Pinto. É. J. D. A. *Hidrologia estatística*. Belo Horizonte: CPRM. 2007.

Oliveira Júnior. A. I.; Martins. E. S.; Costa. C. T. F.; Caldas. H. F. M. Análise da precipitação e determinação de equações de chuvas intensas para o município de Crato-CE situado no semiárido do Brasil. *Revista Geama*. v. 5. n. 3. p. 56-65. 2019.

Silva. G. R.; Oliveira. D. V. C.; Oliveira Junior. A. I.; Carvalho. I. J. 2023. Análise das precipitações pluviométricas do município de Serra Talhada-PE e determinação da equação de chuvas intensas por meio de distribuição probabilística. *Revista de Geografia*. v. 40. n.1. p.306-333. 2023.

Villela. S. M.; Mattos. A. *Hidrologia aplicada*. São Paulo: McGraw-Hill. 1975.